

Intravoxel Incoherent Motion Perfusion Measurement Correlated with DCE-MR Imaging in Prostate Cancer Detection

Yuxi Pang^{1,2}, Baris Turkbey², Marcelino Bernardo^{2,3}, Jochen Kruecker⁴, Samuel Kadoury⁴, Maria J Merino⁵, Bradford Wood⁶, Peter A Pinto⁷, and Peter L Choyke²
¹Philips Healthcare, Cleveland, OH, United States, ²Molecular Imaging Program, National Cancer Institute, Bethesda, Maryland, United States, ³SAIC-Frederick, Bethesda, Maryland, United States, ⁴Philips Research North America, Briarcliff Manor, NY, United States, ⁵Laboratory of Pathology, National Cancer Institute, Bethesda, Maryland, United States, ⁶Diagnostic Radiology Department-Clinical Center, National Institutes of Health, Bethesda, Maryland, United States, ⁷Urologic Oncology Branch, National Cancer Institute, Bethesda, Maryland, United States

Introduction

In recent years¹⁻², there has been renewed interest in intravoxel incoherent motion (IVIM) MR imaging thanks to improved MR hardware performance. According to the IVIM theory, multi b-values diffusion weighted (DW) image measurements are capable of providing not only diffusion but also perfusion information on the tissue of interest. Normally, perfusion information is obtained from dynamic contrast-enhanced (DCE) MRI studies which have shown that tumors tend to have increased perfusion and permeability³. Thus, it is of potential clinical relevance to investigate whether or not IVIM could provide an independent measure of tissue perfusion, without contrast injection. In this retrospective study, we have analyzed 31 DWI and DCE data sets from patients with prostate cancers, and found that both IVIM and DCE derived parameters were equally capable of differentiating prostate tumor from benign tissues, and IVIM-derived perfusion correlated positively with those from DCE measurements.

Methods & Materials

All measurements were performed on a 3T MR scanner (Philips Healthcare, Best, The Netherlands) using a combination of 16-channel SENSE Cardiac Coil with an Endorectal Coil. After T2W TSE scans, an axial DW-MRI was performed using a single-shot spin-echo EPI sequence with the following parameters: TR /TE of 4584/59 ms, FOV (AP/RL/FH) of 160/180/60 mm, number of slices of 20, acquired voxel size of 1.25*1.25*3.00 mm³, b-values of 0, 188, 375, 563,750 s/mm², NSA of either 4 or 8 (for b-values of 563,750 s/mm²), and scan time of 5.9 min. For T1W DCE-MRI, two separate axial scans were acquired - a pre-contrast dry run with a low flip-angle (5°) and a dynamic one with a higher flip-angle (15°) after contrast injection. The temporal resolution of the dynamic scans was either 3 or 5.6 seconds, and scan time was kept within 5 minutes. All patients (N=31) had image-guided biopsy-proven prostate cancers, and lesion malignancy was classified as either high grade (N=16) or low grade (N=15) based on the Gleason score system. On a semi-log plot of pixel signal intensity (*s*) vs. b-values ($\log(s/s_0) = -b \cdot D + \log(1-f)$), diffusion coefficient (*D*) was fitted as the slope with three b-values (188, 375 and 563 s/mm²) images, the fitted data was then extrapolated to obtain the intercept ($\log(1-f)$), which gave the value of perfusion fraction (*f*). An extended Tofts model was used to generate DCE kinetic parameters (*K*_{trans}, *v*_e, and *v*_p). A pre-contrast T1 map and a population-averaged arterial input function (AIF) were included in DCE data modeling. Two ROIs were drawn on the tumor and non-tumor region in DWI and DCE image for each patient, and the corresponding mean and coefficient of variation (%) values of each parameter within all ROI were tabulated for further statistical analysis.

Results & Discussion

Based on IVIM analysis, the population-averaged *D* was significantly (*p* < 0.05) lower in tumors than in normal tissues (see Table 1), while *f* was significantly higher in tumors than in normal tissues, correlating negatively with *D* with a Pearson's coefficient (*r*) of -0.51. From DCE data modeling, *K*_{trans}, *v*_e and *v*_p were all significantly higher in tumors than in normal tissues, consistent with what is known about angiogenesis within tumors; interestingly, *K*_{trans} and *v*_p were positively correlated (*r*=0.51 and 0.46, respectively) with *f*. This positive correlation is exemplified in Figure 1, where the lesion is clearly recognized in the right peripheral zone on both *K*_{trans} (Fig. 1d) and *f* (Fig. 1c) maps; by comparison, the same lesion is hypointense on the T2W image (Fig. 1a) and diffusion coefficient map (Fig. 1b). To extract both diffusion and perfusion information from a single diffusion acquisition based on IVIM is of potential clinical relevance. One appealing feature of this data is that perfusion information might be obtained without the need for intravenous contrast media. This is especially relevant in patients with compromised renal function or severe allergies who cannot receive intravenous gadolinium-based contrast media. In summary, we showed that both IVIM and DCE parameters were equally capable of differentiating prostate tumor from benign tissues, and raised the possibility of eliminating DCE-MRI in the multi-parametric paradigm for diagnosing prostate cancer with MRI.

Parameters	Normal	Tumor	t-Test
<i>D</i> (10 ⁻³ mm ² /s)	1.76 ± 20%	0.99 ± 30%	<i>p</i> < 0.05
<i>f</i> (%)	3.7% ± 52%	7.2% ± 37%	<i>p</i> < 0.05
<i>K</i> ^{trans} (min ⁻¹)	0.18 ± 55%	0.39 ± 56%	<i>p</i> < 0.05
<i>v</i> _e (%)	26% ± 42%	32% ± 44%	<i>p</i> < 0.05
<i>v</i> _p (%)	3.4% ± 75%	8.4% ± 78%	<i>p</i> < 0.05

Table 1: Diffusion coefficients (*D*) and perfusion fractions (*f*), and *K*_{trans}, *v*_e and *v*_p are expressed as mean ± coefficient of variation (%). The separation between normal and tumor tissues for each parameter is characterized by the *p*-value from Student's *t*-test.

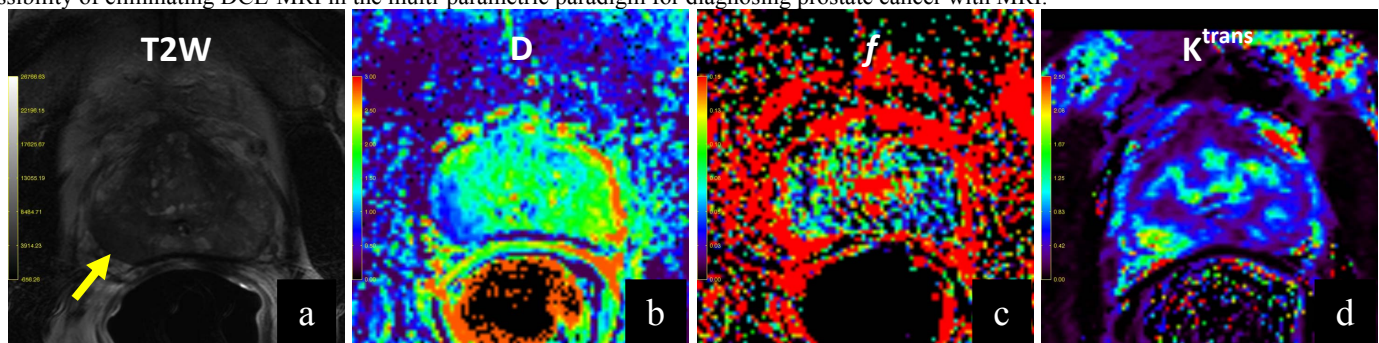


Figure 1 (a-d): (a) T2W image; (b) Diffusion coefficient image; (c) Perfusion fraction (*f*) image; and (d) *K*_{trans} image. A lesion was located in the right peripheral zone indicated by a yellow arrow in (a).

References

- (1). Luciani A, et al. Radiology 2008; 249 (3): 891-899.
- (2). Riches SF, et al. NMR in Biomedicine 2009; 22(3): 318-325.
- (3). Ocak I, et al. AJR Am J Roentgenol 2007;189(4):849.